

CHEMISTRY

A European Journal

A Journal of



Accepted Article

Title: Rotating iron and titanium sandwich complexes

Authors: Filip Vlahovic, Maja Gruden, and Marcel Swart

This manuscript has been accepted after peer review and appears as an Accepted Article online prior to editing, proofing, and formal publication of the final Version of Record (VoR). This work is currently citable by using the Digital Object Identifier (DOI) given below. The VoR will be published online in Early View as soon as possible and may be different to this Accepted Article as a result of editing. Readers should obtain the VoR from the journal website shown below when it is published to ensure accuracy of information. The authors are responsible for the content of this Accepted Article.

To be cited as: *Chem. Eur. J.* 10.1002/chem.201704829

Link to VoR: <http://dx.doi.org/10.1002/chem.201704829>

Supported by
ACES

WILEY-VCH

Rotating iron and titanium sandwich complexes

Filip Vlahovic^a, Maja Gruden^b, Marcel Swart^{c,d}

Abstract: The origin for the rotational barrier of organometallic vs inorganic sandwich complexes has remained enigmatic for the past decades. Here, we investigate in detail what causes the substantial barrier for titanodecaphosphacene through spin-state consistent density functional theory. Orbital interactions are shown to be the determining factor.

Recently a challenge was put forward on Twitter¹ to get a better understanding for the difference observed² in the rotational barrier of ferrocene (**Fc**, [Fe^{II}(C₅H₅)₂]⁰) vs. titanodecaphosphacene (**TdP**, [Ti⁰(P₅)₂]²⁻), with values of respectively ca. 1 kcal·mol⁻¹ (**Fc**) vs. ca. 8 kcal·mol⁻¹ (**TdP**). The cyclo-P₅ anionic ring is the inorganic analogue of the cyclopentadienyl ring and is known to form complexes with several (transition) metals.²⁻⁸ Both compounds fall within the category of sandwich complexes,⁹ which since the discovery of ferrocene^{10, 11} has led to a complete new field within organometallic chemistry. In both cases the central metal is coordinated on both sides to a five-membered anionic ring (see Figure 1), whose idealized structure can exist in either D_{5d} or D_{5h} symmetry. There had been discussion about which one of the conformers would be the most stable one for **Fc**, because the difference in energy was too small to measure experimentally. Based on more precise experimental methods it was found that the eclipsed D_{5h} conformer of Fe^{II} in the low spin state (S=0) dominates in the vapor state^{12, 13}, which was confirmed by theoretical chemistry;¹⁴⁻¹⁶ the same conformer was found to prevail for **TdP**.² Surprisingly, a major difference was observed for the barrier heights.^{2, 17} Here, we address the challenge that was put forward for understanding the stability and interconversion of the rotamers of these sandwich complexes, with density functional theory (DFT) calculations. Through the use of spin-state consistent density functional approximations¹⁸ and chemical bonding analyses,¹⁹ we have determined what causes the surprisingly large difference in rotational barrier.

The first step in our study was the optimization of the structures of the D_{5d} and D_{5h} conformers for both compounds at OPBE/TZP²⁰ (including ZORA²¹ relativistic corrections). For both conformers, the sandwich complexes in both D_{5h} and D_{5d}

arrangement adopt stacking structures due to the ligand's π-orbitals and its aromaticity.^{2, 22}

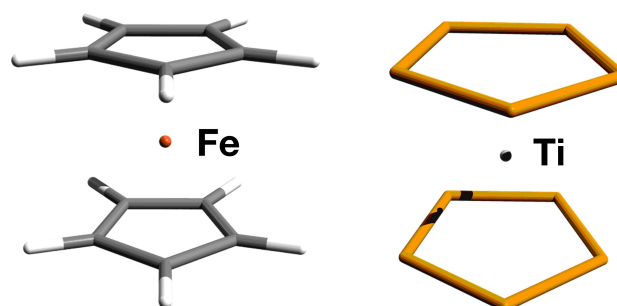


Figure 1. Structure of ferrocene (**Fc**) and titanodecaphosphacene (**TdP**)

Our calculations confirm that indeed the D_{5h} conformation is a true global minimum for both **Fc** and **TdP**, without any imaginary frequencies (see Table 1). Our calculations also revealed that the staggered (D_{5d}) conformation is in both cases a saddle point, corroborating previous theoretical studies.¹⁴⁻¹⁶ The obtained structural parameters for the two conformers D_{5h} and D_{5d} (see Table S1) are nearly identical for **Fc** and slightly different for **TdP**. Furthermore, we performed separate optimizations for the three possible spin states (low, intermediate, high), which indicated clearly that the low-spin S=0 spin-state is in all cases the spin ground state, with the other spin states more than 30 kcal·mol⁻¹ higher in energy (Table S2).

Our calculations showed that for both conformers, the frontier MOs are constructed from nearly the same amount of metal and ligand orbitals. The differences between the HOMOs and LUMOs are not significant enough to differentiate between the conformers (Table 1), and therefore we had to focus our attention on chemical bonding analyses.

Chemical bonding analysis Fc. We start our analysis on the origin of the barrier with the Energy Decomposition Analysis (EDA)¹⁹ which had been shown to be very useful in the past.²³ The structural resemblance between the conformers (*vide supra*) allowed us to explore the change of energy, and factors contributing to it. This was used as function of the rotation of one ring relative to the other, whereby we can neglect the change in the geometry of the ligand and/or metal-ligand distance. We chose to perform the rotation in both **Fc** and **TdP** in steps of 5 degrees starting from the more stable (D_{5h}, dihedral angle of 0 degrees) and going to the less stable (D_{5d}, dihedral angle of 180 degrees) conformation, see Figure 2.

At every point of the rotation we performed an EDA analysis in order to follow the energy change in a way that can give us more information about the factors that are contributing to the stability. The EDA analysis has been used to calculate the energy components that contribute to the overall energy in a chemical sense. The destabilizing Pauli repulsion (ΔE_{Pauli}) is larger in the D_{5h} conformer than in D_{5d}, for both **Fc** and **TdP**; this obviously makes sense since the distance between CH or P units on the opposite side of the metal are slightly larger within the staggered D_{5d} conformation.

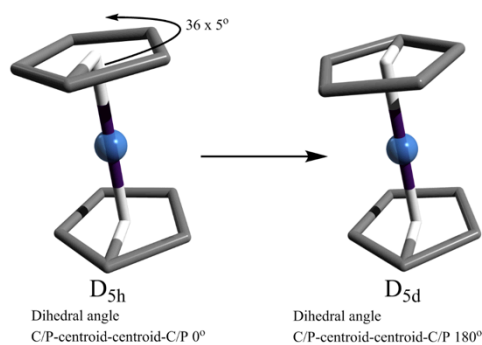
- [a] Filip Vlahovic
Innovation center of the Faculty of Chemistry
University of Belgrade
Studentski trg 12–16, 11000 Belgrade, Serbia
- [b] Dr. Maja Gruden
Faculty of Chemistry
University of Belgrade
Studentski trg 12–16, 11000 Belgrade, Serbia
- [c] Prof. Dr. Marcel Swart
Institut de Química Computacional i Catalisi
University of Girona
Campus Montilivi (Ciències), 17003 Girona, Spain
- [d] Prof. Dr. Marcel Swart
ICREA
Pg. Lluís Companys 23, 08010 Barcelona, Spain
E-mail: marcel.swart@icrea.cat

Supporting information for this article is given via a link at the end of the document, and at iochem-bd.org repository.

Table 1. Energy (ZORA/OPBE/TZP) for two conformers of Fc and TdP

	Fc			TdP		
	D _{5d}	$\Delta(D_{5d} - D_{5h})$	D _{5h}	D _{5d}	$\Delta(D_{5d} - D_{5h})$	D _{5h}
E(electronic) ^a	1.41		0	5.99		0
HOMO-LUMO ^b	3.172	-0.085	3.228	1.796	-0.158	1.954
EDA						
ΔE_{prep}	239.90	-1.10	241.00	237.56	-5.18	242.74
ΔE_{deform}	1.40	-0.22	1.62	4.58	-1.18	5.76
$\Delta E_{\text{cyc-cyc}}$	102.79	-0.88	103.67	87.28	-4.00	91.28
ΔE_{valexc}	135.71	0.00	135.71	145.7	0.00	145.7
ΔE_{elstat}	-619.73	0.78	-620.51	-261.33	19.67	-281
ΔE_{Pauli}	345.63	-3.28	348.91	327.3	-28.15	355.45
ΔE_{orbint}	-631.66	5.00	-636.66	-434.09	19.67	-453.76
a_{1g} / a_1'	-53.19	0.14	-53.33	-15.55	0.07	-15.62
e_{1g} / e_1''	-394.31	3.01	-397.32	-52.10	1.37	-53.47
e_{1u} / e_1'	-66.99	0.62	-67.61	-4.03	-0.15	-3.88
a_{2u} / a_2''	-31.00	0.10	-31.10	-4.62	-0.01	-4.61
e_{2g} / e_2'	-67.68	1.45	-69.13	-356.44	18.27	-374.71
e_{2u} / e_2''	-18.50	-0.32	-18.18	-1.34	0.12	-1.46
E_{total}	-665.86	1.40	-667.26	-130.56	6.01	-136.57

a) kcal·mol⁻¹; b) eV

**Figure 2.** Gradual rotation of one ring relative to the other in steps of 5 degrees leads to the change of dihedral angle from 0° to 180° and at the same time to the interconversion of D_{5h} to D_{5d} conformer.

At the same time, it is accompanied by a larger favorable electrostatic interaction (ΔE_{elstat}) in the D_{5h} conformer, which partially compensates for the difference in Pauli repulsion. However, the sum of these two components (sometimes called steric interactions) is favoring the D_{5d} conformer. It is only by taking into account the orbital interactions (ΔE_{orbint}) that D_{5h} emerges as the most stable conformer. In order to understand better the origin of these differences in orbital interactions, we

further decomposed the ΔE_{orbint} into contributions resulting from the different irreps.

The main orbital set responsible for the larger ΔE_{orbint} in Fc is coming from the doubly degenerate orbitals of e_1' symmetry (equivalent to e_{1g} orbitals in D_{5d}). A detailed analysis of these orbitals revealed that they consist mostly of filled bonding ligand orbitals (~70%) with empty non-bonding counterparts mainly from metal *d* orbitals. If we take a look at these orbitals (Figure 3) we see similar bonding patterns for both D_{5d} and D_{5h}, but slightly better overlapping for the latter.

Now that we identified the main source for the stability of the D_{5h} conformer (ΔE_{orbint}), we performed the rotation of one ring relative to the other. We observed that the change in total bonding energy along this rotation was determined mainly by ΔE_{orbint} . Our EDA analysis showed a smooth wave-like energy profile with the total ΔE_{orbint} oscillating between the values for the D_{5h} (at 0°) and D_{5d} (at 180°) conformers (see Fig. 4).

Note that the ΔE_{orbint} energy for (D_{5h}-frozen) "D_{5d}" differs from the value for the D_{5d}-optimized conformer (see Table S3). Of course, if we allow the D_{5h}-frozen "D_{5d}" structure to relax, it will reach the true minimum within D_{5d} symmetry, which is only 0.05 kcal·mol⁻¹ lower in energy. This value is however obtained through rebalancing of Pauli repulsion (which gets smaller by 2.83 kcal·mol⁻¹) and orbital interactions (which gets less favorable by 2.79 kcal·mol⁻¹) energies. Therefore, we can conclude that the somewhat larger metal to ring-center distance

in case of D_{5d} conformer (Table S1) is resulting from the relief of Pauli repulsion, which simultaneously is counteracted by a loss of favorable orbital interactions.

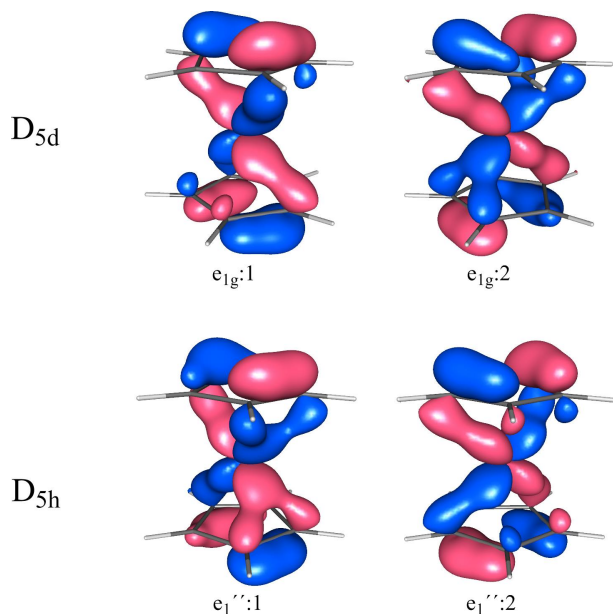


Figure 3. Doubly degenerate orbitals responsible for stabilization of the eclipsed (D_{5h}) and staggered (D_{5d}) arrangements of ferrocene.

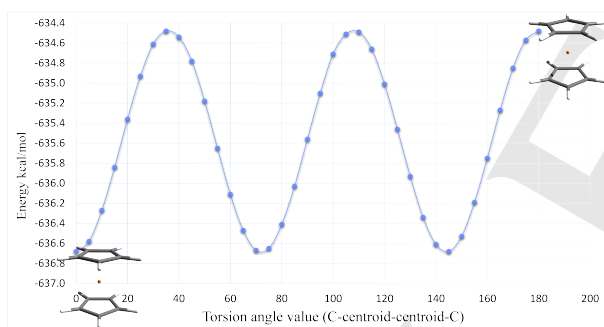


Figure 4. Change of the total ΔE_{orbint} during the rotation of one ring relative to the other in steps of 5 degrees, starting from D_{5h} (dihedral C-centroid-centroid-C of 0°) and going to the D_{5d} (dihedral angle 180°) conformation

Chemical bonding analysis TdP. Although **Fc** and **TdP** are both sandwich complexes, there are critical differences in these (in)organic complexes. The rotation barrier for **TdP** is $5.99 \text{ kcal}\cdot\text{mol}^{-1}$ (at OPBE/TZP, see Table 1), while the barrier for **Fc** is only $1.41 \text{ kcal}\cdot\text{mol}^{-1}$. This might be attributed to the barriers increasing upon larger metal π -donation (backdonation).²⁴ However, the structural parameters (Table S1) show drastically larger Ti-P distances (2.53 \AA) compared to Fe-C (2.00 \AA), which results mainly from the P_5^- ring itself (P-P 2.15 \AA). Also the metal-centroid bond is affected (**Fc** 1.59 \AA , **TdP** 1.74 \AA). Moreover, these distances are larger for D_{5d} than for D_{5h} (see Table S1). Hence, the metal π -donation would be expected to be counteracting the rotational barrier.

The EDA analysis shows that although the absolute value of ΔE_{orbint} is smaller for **TdP** than for **Fc** (Table 1), the *difference* between D_{5h} and D_{5d} is much larger ($19.7 \text{ kcal}\cdot\text{mol}^{-1}$ for **TdP** vs. $5 \text{ kcal}\cdot\text{mol}^{-1}$ for **Fc**). The steric interactions (sum of ΔE_{elstat} and ΔE_{Pauli}) varies much less ($2.5 \text{ kcal}\cdot\text{mol}^{-1}$ for **Fc**, $8.5 \text{ kcal}\cdot\text{mol}^{-1}$ for **TdP**), even though the individual components do vary. The destabilizing Pauli repulsion (which favors D_{5d}) can be attributed to an electronic effect, where electron-accepting character on the ligands facilitates removal of electron density from Ti. At the same time it boosts the effect of the lone pairs on the P atoms.

The decomposition of ΔE_{orbint} into the contributions from the irreps for **TdP** shows a difference with the results for **Fc**. The main orbital set responsible for the larger ΔE_{orbint} in D_{5h} arrangement is now coming from the doubly degenerate orbitals of e_2' symmetry. Unlike the case of **Fc**, these **TdP** orbitals consist mostly of empty antibonding ligand orbitals ($\sim 80\%$) with filled non-bonding counterpart originating from metal d orbitals. However, the most drastic change when going from D_{5h} to D_{5d} in **TdP** is the reorientation of the density, which moves from "cis"-like pattern in D_{5h} for $e_2':1$ (with a larger overlap), to "trans"-like in D_{5d} ($e_{2g}:1$); compare e.g. the blue lobes in the Fig. 5 (left), together with the corresponding participation of P-orbitals (in pink). This is in sharp contrast to the situation for **Fc**, where the shape of the orbitals responsible for the ΔE_{orbint} difference hardly change during the rotation from D_{5h} to D_{5d} (see Figure 3).

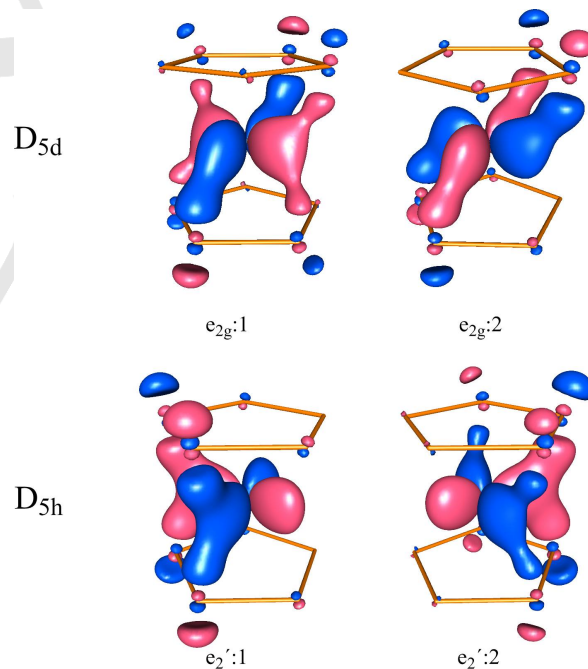


Figure 5. Doubly degenerate orbitals responsible for stabilization of the eclipsed (D_{5h}) and staggered (D_{5d}) arrangements of **TdP**

The origin for the larger rotational barrier in **TdP** vs. **Fc** is therefore resulting from orbital interactions (ΔE_{orbint}). In particular the changes in the orbitals in the e_2' irrep, perhaps due to smaller overlap because of larger metal-ligand distances, which comes with an energetic cost because of a smaller overlap in D_{5d} which inherently favours the D_{5h} arrangement of **TdP**.

Experimental Section

DFT calculations have been carried out using QUILD²⁵ and the Amsterdam Density Functional program (ADF2016.01).^{26, 27} Geometry optimizations were performed using the OPBE functional,^{20, 28, 29} including ZORA²¹ scalar relativistic corrections, in a triple-zeta basis set with one polarization (TZP) of Slater type orbitals.^{30, 31} For all calculations the Becke grid of verygood quality was used.^{32, 33} Chemical bonding analyses (EDA¹⁹) were carried out (see Supporting Information).

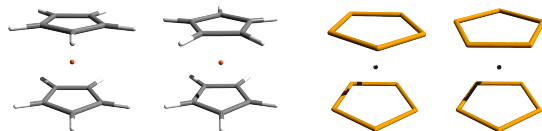
Acknowledgements

The following organizations are thanked for financial support: MINECO (projects CTQ2014-59212-P and CTQ2015-70851-ERC), GenCat (project 2014SGR1202, and XRQTC network), MICINN and European Fund for Regional Development (UNGI10-4E-801), and the Serbian Ministry of Science (Grant No. 172035). This work was performed in the framework of COST Action CM1305 "Explicit Control Over Spin-states in Technology and Biochemistry (ECOSTBio)" (STSM reference: COST-STSM-CM1305-38408).

Keywords: spin states • sandwich compounds • density functional approximations • ferrocene • chemical bonding

1. C. J. Cramer, 2016, vol. 2016.
2. E. Urnežiū, W. W. Brennessel, C. J. Cramer, J. E. Ellis and P. v. R. Schleyer, *Science*, 2002, 295, 832-834.
3. M. Baudler, *Angew. Chem. Int. Ed.*, 1987, 26, 419-441.
4. B. M. Gimarc, *Pure Appl. Chem.*, 1990, 62, 423.
5. O. J. Scherer, T. Brück and G. Wolmershäuser, *Chem. Ber.*, 1988, 121, 935-938.
6. Alexander R. Kudinov, Dmitry A. Loginov, Zoya A. Starikova, Pavel V. Petrovskii, M. Corsini and P. Zanello, *Eur. J. Inorg. Chem.*, 2002, 2002, 3018-3027.
7. M. Baudler and K. Glinka, *Chem. Rev.*, 1993, 93, 1623-1667.
8. A. Castro, E. Osorio, J. L. Cabellos, E. Cerpa, E. Matito, M. Solà, M. Swart and G. Merino, *Chem. Eur. J.*, 2014, 20, 4583-4590.
9. J. I. Seeman and S. Cantrill, *Nat Chem*, 2016, 8, 193-200.
10. T. J. Kealy and P. L. Pauson, *Nature*, 1951, 168, 1039-1040.
11. S. A. Miller, J. A. Tebboth and J. F. Tremaine, *J. Chem. Soc.*, 1952, 1952, 632-635.
12. E. R. Lippincott and R. D. Nelson, *Spectrochim. Acta*, 1958, 10, 307-329.
13. R. K. Bohn and A. Haaland, *J. Organomet. Chem.*, 1966, 5, 470-476.
14. N. Mohammadi, A. Ganesan, C. T. Chantler and F. Wang, *J. Organomet. Chem.*, 2012, 713, 51-59.
15. S. Coriani, A. Haaland, T. Helgaker and P. Jørgensen, *ChemPhysChem*, 2006, 7, 245-249.
16. T. P. Gryaznova, S. A. Katsyuba, V. A. Milyukov and O. G. Sinyashin, *J. Organomet. Chem.*, 2010, 695, 2586-2595.
17. Y. Yamaguchi, W. Ding, C. T. Sanderson, M. L. Borden, M. J. Morgan and C. Kutal, *Coord. Chem. Rev.*, 2007, 251, 515-524.
18. M. Swart and M. Gruden, *Acc. Chem. Res.*, 2016, 49, 2690-2697.
19. F. M. Bickelhaupt and E. J. Baerends, in *Reviews in Computational Chemistry*, Vol 15, Wiley-VCH, New York, 2000, vol. 15, pp. 1-86.
20. M. Swart, A. W. Ehlers and K. Lammertsma *, *Molec. Phys.*, 2004, 102, 2467-2474.
21. E. van Lenthe, E. J. Baerends and J. G. Snijders, *J. Chem. Phys.*, 1993, 99, 4597-4610.
22. D. E. Bean, P. W. Fowler and M. J. Morris, *J. Organomet. Chem.*, 2011, 696, 2093-2100.
23. M. Swart, *Inorg. Chim. Acta*, 2007, 360, 179-189.
24. M. Bochmann, *Organometallics*, Oxford Univ. Press, New York, 1994.
25. M. Swart and F. M. Bickelhaupt, *J. Comput. Chem.*, 2008, 29, 724-734.
26. G. te Velde, F. M. Bickelhaupt, E. J. Baerends, C. Fonseca Guerra, S. J. A. van Gisbergen, J. G. Snijders and T. Ziegler, *J. Comput. Chem.*, 2001, 22, 931-967.
27. E. J. Baerends, T. Ziegler, A. J. Atkins, J. Autschbach, D. Bashford, A. Bérces, F. M. Bickelhaupt, C. Bo, P. M. Boerrigter, L. Cavallo, D. P. Chong, D. V. Chulhai, L. Deng, R. M. Dickson, J. M. Dieterich, D. E. Ellis, M. v. Faassen, L. Fan, T. H. Fischer, C. Fonseca Guerra, M. Franchini, A. Ghysels, A. Giammona, S. J. A. van Gisbergen, A. W. Götz, J. A. Groeneveld, O. V. Gritsenko, M. Grüning, S. Gusarov, F. E. Harris, T. Heine, P. van den Hoek, C. R. Jacob, H. Jacobsen, L. Jensen, J. W. Kaminski, G. van Kessel, F. Kootstra, A. Kovalenko, M. V. Krykunov, E. van Lenthe, D. A. McCormack, A. Michalak, M. Mitoraj, S. M. Morton, J. Neugebauer, V. P. Nicu, L. Noodleman, V. P. Osinga, S. Patchkovskii, M. Pavanello, C. A. Peebles, P. H. T. Philipsen, D. Post, C. C. Pye, W. Ravenek, J. I. Rodríguez, P. Ros, R. Rüger, P. R. T. Schipper, H. van Schoot, G. Schreckenbach, J. S. Seldenthuis, M. Seth, J. G. Snijders, M. Solà, M. Swart, D. Swerhone, G. te Velde, P. Vermooijs, L. Versluis, L. Visscher, O. Visser, F. Wang, T. A. Wesolowski, E. M. van Wezenbeek, G. Wiesenecker, S. K. Wolff, T. K. Woo and A. L. Yakovlev, *ADF2016*, (2016) SCM, Theoretical Chemistry, Vrije Universiteit, Amsterdam.
28. N. C. Handy and A. J. Cohen, *Molec. Phys.*, 2001, 99, 403-412.
29. J. P. Perdew, K. Burke and M. Ernzerhof, *Phys. Rev. Lett.*, 1996, 77, 3865-3868.
30. E. Van Lenthe and E. J. Baerends, *J. Comput. Chem.*, 2003, 24, 1142-1156.
31. D. P. Chong, E. Van Lenthe, S. Van Gisbergen and E. J. Baerends, *J. Comput. Chem.*, 2004, 25, 1030-1036.
32. M. Franchini, P. H. T. Philipsen and L. Visscher, *J. Comput. Chem.*, 2013, 34, 1819-1827.
33. A. D. Becke, *J. Chem. Phys.*, 1988, 88, 2547-2553.

COMMUNICATION



Origin of rotational barriers in ferrocene vs. titanododecaphosphacene

*F. Vlahovic, M. Gruden, M. Swart**

Page No. – Page No.

Rotating iron and titanium sandwich complexes